Numerical Simulation of Gliding Arc Plasma Motion Characteristics

Mengfei Yang[1], Zongyu Wang[2,3](✉), Wei Zhang[1], Jifeng Zhang[1,2], Hai Zhang[3], and Yulong Ji[1]

[1] College of Marine Engineering, Dalian Maritime University, Dalian 116206, China
jiyulong@dlmu.edu.cn
[2] Yangtze Delta Region Institute of Tsinghua University Zhejiang, Jiaxing 314006, China
wangzongyu09@163.com
[3] College of Energy and Power Engineering, Tsinghua University, Beijing 100084, China

Abstract. In this paper, a mathematical model of DC gliding arc plasma was established based on magneto-hydrodynamic theory (MHD), and the finite element software COMSOL was used to solve the coupling process of electromagnetic field, temperature field and velocity field. The effects of flow rate, electrode throat and voltage on the gliding arc velocity, temperature and current density distribution were studied. The results show that the gliding arc discharge presents a cyclic process of arc breakdown, elongation, disappearance, and re-breakdown. The flow rate has a significant effect on the arc characteristic distribution, and the gas blowing makes the arc discharge appear "arc shape". When arc breakdown, the arc temperature and current density have the maximum value at the electrode. As the arc gradually stabilizes to form an arc column, the maximum moves to the center of the arc column and gradually decreases along the radial direction. As the flow rate increases, the maximum velocity increases, while the temperature and current density decreases. With the electrode throat gap narrowing, the temperature and current density reach the maximum quickly. It only needs 0.4 ms to reach the maximum when gap is 2 mm. And the smaller the gap, the easier it is for the arc to re-breakdown. The temperature and current density increase with the voltage. This work reveals the motion characteristics of the gliding arc between the electrodes. The influence of characteristic parameters on gliding arc plasma is clarified. It provides a certain basis for optimizing the structure of the gliding arc reactor.

Keywords: Gliding arc discharge · Plasma · MHD · Multiphysics · Movement characteristics

1 Introduction

Plasma, a system composed of a large number of charged and neutral particles, has received much attention in recent years and plays an important role in biomedicine [1], materials processing [2, 3], energy conversion [4, 5], pollutant degradation [6, 7], and environmental protection [8]. At present, the more mature low-temperature plasma jet

D. Dai et al. (Eds.): ISPEC 2022, SPPHY 391, pp. 339–351, 2023.
https://doi.org/10.1007/978-981-99-1576-7_32

and jet array technologies have good treatment effects in the above-mentioned fields. However, they have the disadvantages of small treatment area and uneven treatment area. The gliding arc discharge (GAD), as a way to generate plasma at atmospheric pressure [9], has a simple generation device, long electrode life, and a wide operating range (i.e., pressure range is Torr-atm and above, and the arc current is mA–A). It can generate a wide plasma in open space, thus increasing the plasma treatment area and improving the treatment efficiency. It has been successfully applied to plasma-assisted gas treatment in chemical and environmental protection fields [10, 11].

Many researchers have done a great deal of research on gliding arc plasma because of its broad range of applications and exceptional benefits. In terms of experiment, He et al. [12] investigated the effects of electrode expansion angle and air flow rate on the gliding arc discharge characteristics, and examined the influence of power supply voltage magnitude on the development of the accompanying breakdown gliding discharge mode to the stable gliding discharge mode. Sun et al. [13] explored the effect of air gas flow rate on the percentage of the two modes. Chen et al. [9] studied the effect of different gas composition addition on the nitrogen gliding arc discharge. Sun et al. [14] analyzed the arc motion mode of gliding arc. In terms of numerical simulation, Wang et al. [15] studied the discharge characteristics of the gliding arc. The results show that the arc axis temperature could reach 5700–6700 K. Zhao et al. [16] used magneto-hydrodynamic theory to establish the mathematical model of DC arc plasma and simulated the characteristics of the multi-physics field distribution of the arc plasma. Liu et al. [17] compared the characteristics of AC and DC vacuum arc plasma and found that the AC arc and DC arc plasma parameters distribute similarly under the same current excitation. And the AC arc is easier to be opened and broken because its energy decreases faster. Chen et al. [18] studied the numerical simulation of DC arc plasma torch and found that the highest value of the plasma temperature appeared near the cathode and decreased with the axial distance. The working gas flow rate has little effect on the temperature distribution inside the torch.

At present, most of the numerical simulations are carried out only for the arc plasma torch. It has fewer simulations for the physical characteristics of the two-dimensional gliding arc, transient motion processes, etc. Therefore, in order to better understand the motion characteristics of the gliding arc, this paper constructed a two-dimensional model of the gliding arc discharge plasma by the magneto-hydrodynamic equation. The motion characteristics of the sliding arc between the electrodes was simulated. The influence of the characteristic parameters on the gliding arc plasma was clarified. It provides a certain basis for optimizing the structure of the sliding arc reactor.

2 Arc Modeling and Simulation

2.1 Geometry Model

The simulation geometry model used in this paper is shown in Fig. 1. A knife-shaped copper electrode model is used, setting AF as the cathode, BC as the anode, AB as the fluid inlet and DE as the fluid outlet. The electrode throat is set as 2–6 mm.

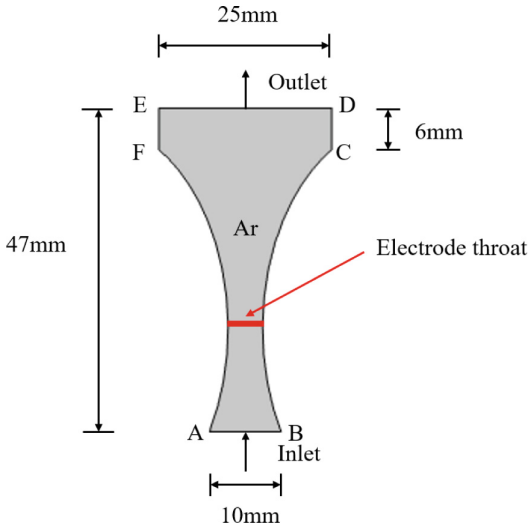

Fig. 1. Gliding arc simulation geometry model

2.2 Model Assumptions

The arc can usually be divided into three parts, namely cathode area, arc column area and anode area [19]. The generation of the arc plasma is an extremely complex process. In order to simplify the computational process and reduce the complexity of the simulation analysis, the following assumptions are made [20–23]:

1) The arc plasma is in local thermodynamic equilibrium state.
2) The gas density, viscosity, specific heat capacity, thermal conductivity, electrical conductivity and other physical parameters are only a function of temperature.
3) The arc plasma is a constant flow and two-dimensional distribution.
4) The plasma arc is in a laminar flow state and incompressible.
5) The influence of the sheath layer in the electrode region is ignored.

2.3 Boundary Conditions

The simulation boundary conditions are set as follows.

1) Fluid heat transfer conditions: The electrode is set as solid. The fluid is set as argon. The inlet and outlet temperatures of the fluid domain are set as 293.15 K. And the rest of the surface is thermally insulated.
2) Pressure boundary conditions: The upper boundary is set as the fluid outlet with a pressure value of 1 atm. The lower boundary is the fluid inlet with different inflow velocities. The electrode boundary is set as a non-slip boundary condition.
3) Voltage boundary conditions: The left electrode boundary is set as cathode. The right electrode boundary is set as anode. A DC voltage is applied to the cathode, and the ballast resistance Rb is set as 1000 Ω. Current conservation is observed in all areas. And the whole outer boundaries are electrically insulated.

2.4 Simulation Scheme

The following simulation calculation scheme was used to examine the impacts of inlet gas flow rate, electrode throat, and excitation voltage on the features of the arc parameters (Table 1).

Table 1. Simulation scheme

number	Inlet gas flow rate (m/s)	Electrode throat (mm)	Excitation voltage (V)
1	3, 5, 7, 9	5	3700
2	5	2, 3, 4, 5, 6	3700
3	5	5	3500, 3600, 3700, 3800, 3900, 4000

3 Results and Discussions

3.1 Simulation Model Validation

Figure 2 shows the shape of the gliding arc discharge and the change of its motion process when the electrode throat is 2 mm and the inlet gas flow rate is 5 m/s. Arc breakdown, elongation, disappearance, and re-breakdown are all observed. Firstly, a short conductive path is formed in the electrode throat, that is, the arc breakdown. And then the arc slides upward along the electrode and arc is gradually elongated. This process is called arc elongation. Finally, the arc breaks and disappears. And a conductive path appears at the electrode throat. This process is essentially identical with the arc discharge shape captured by high-speed photography in the literatures [24, 25], demonstrating the accuracy of the model presented in this research.

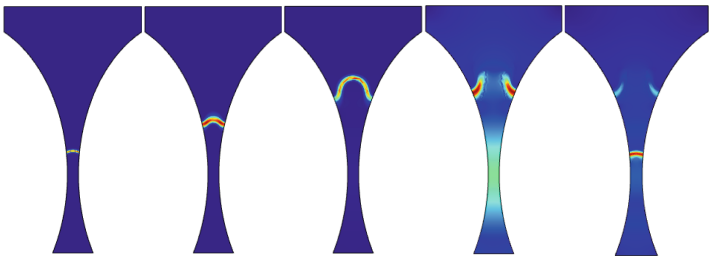

Fig. 2. Gliding arc discharge process

3.2 Velocity Field

Figure 3 shows the maximum inter-electrode velocity versus time curves for different inlet gas rates, different electrode throats and different excitation voltages for the blade type electrodes. The variation of inter-electrode maximum velocity with time for different inlet gas flow rates at 5 mm electrode throat and 3700 V excitation voltage is shown in Fig. 3a. The results show that the larger the inlet flow rate, the bigger the maximum velocity between electrodes. The maximum velocity between electrodes can reach 21 m/s when the inlet flow rate is 9 m/s. When the excitation voltage is 3700 V and the inlet flow rate is 5 m/s, the maximum velocity between electrodes under different electrode throats varies with time as shown in Fig. 3b. The maximum velocity between electrodes increases with the electrode throat spacing. This is because the shortening of the electrode throat increases the degree of gas flow compression, which leads to the increase of velocity. When the spacing is 2 mm, the maximum velocity shows a periodic change, which is mainly due to the arc re-breakdown and it will be analyzed in detail later. When the inlet air flow rate is 5 m/s and the electrode throat is 5 mm, the maximum velocity between electrodes with different excitation voltages varies with time as shown in Fig. 3c, and it is found that the voltage has almost no obvious effect on the maximum velocity, which may be caused by the small excitation voltage range selected. In order to further investigate whether the excitation voltage influences the velocity, this paper also selected a voltage

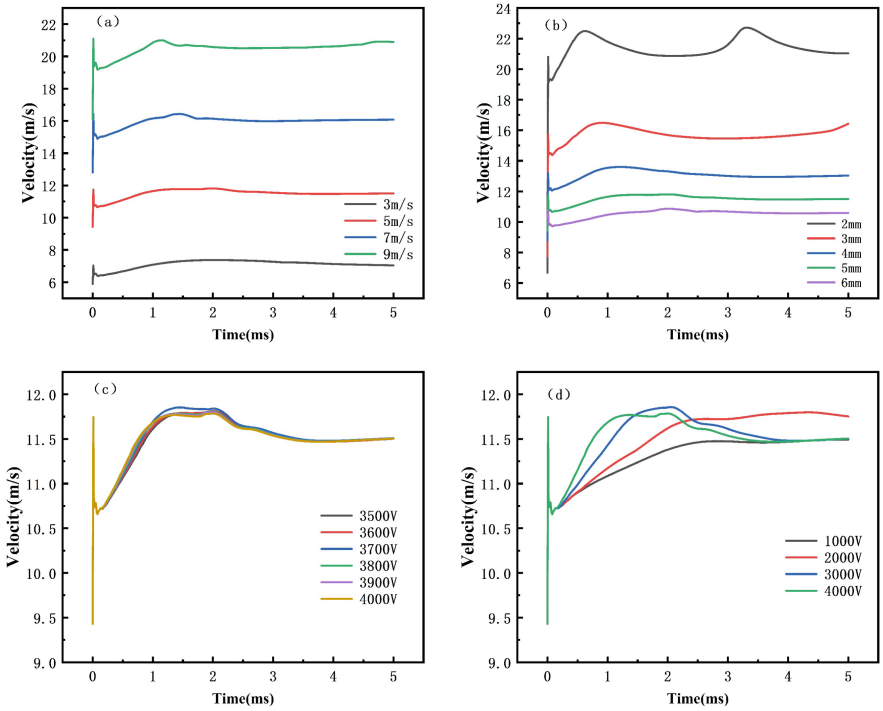

Fig. 3. Plot of the maximum velocity versus time. (a) different inlet gas rates; (b) different electrode throats; (c–d) different voltages

of 1000–4000 V for simulation calculation, as shown in Fig. 3d, the results show that the larger the voltage, the faster the maximum velocity is reached.

In order to observe the maximum velocity change between the electrodes more intuitively, the velocity streamline distribution cloud diagram is given when the inlet flow velocity is 9 m/s, the electrode throat spacing is 5 mm, and the excitation voltage is 3700 V, shown as Fig. 4a. The fluid velocity in the throat presents the maximum, about 21 m/s. With the increase of time, the velocity distribution is similar to the jet. And the velocity gradually decreases along the radial direction at the tail of the flow. The flow process of fluid between electrodes can be regarded as in the Laval nozzle. Due to fluid inertia, the fluid mass does not immediately adhere to the wall, but leaves the wall at the sudden expansion of the pipe. Therefore, a vortex flow appears [26]. Figure 4b shows the isobaric distribution cloud. It shows that there is a pressure difference at the throat. And under the action of the pressure difference, the fluid accelerates along the direction of the pressure gradient. So the velocity is maximum at the throat.

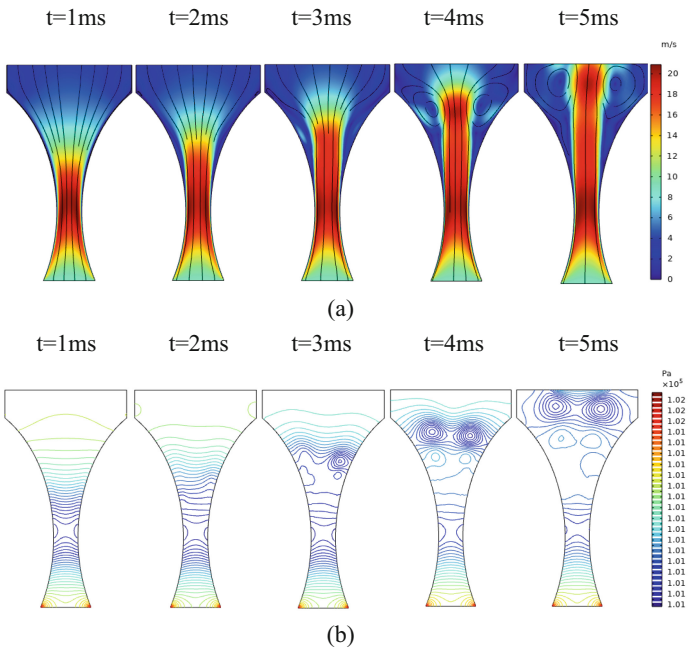

Fig. 4. (a) Velocity flow line distribution cloud (b) Isobaric distribution cloud

3.3 Temperature Field

The arc temperature generally in the range of 3000–20000 K [16, 18, 27–29], is one of the important parameters of the arc. The maximum arc temperature calculated by the model in this paper is about 7500 K, which verifies the correctness of the model. Figure 5 depicts the graphs of the maximum temperature between the blade electrodes with time

for different inlet flow rates, different electrode throats, and different excitation voltages. It can be seen that the arc temperature basically reaches the maximum value within 1 ms and then is keeps in a relatively stable state. This is because after the voltage is applied to the electrodes, the argon between the electrodes is ionized by strongly heated. And under the action of electric field, the cation moves toward the cathode, and the anion and free electron move toward the anode. A large number of strong particle collisions occur, resulting in a high temperature arc between the electrodes. Subsequently, the arc is in a stable burning state under the maintenance of voltage.

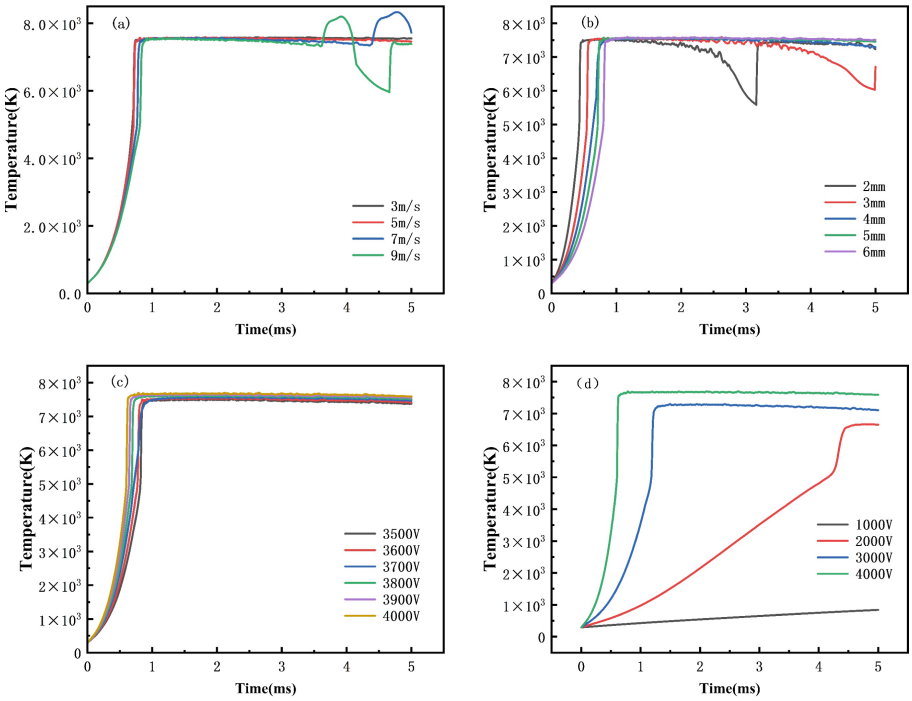

Fig. 5. Plot of maximum temperature versus time (a) different inlet flow rates (b) different electrode throats (c–d) different voltages

When the electrode throat is 5 mm and excitation voltage is 3700 V, different inlet gas flow rate between the electrode maximum temperature change with time is shown in Fig. 5a. When the inlet gas flow rate is 9 m/s, the arc temperature will appear large fluctuation, in 3.7 ms–4.7 ms.It is caused by the arc re-breakdown. When the flow rate is 7 m/s, it also begins to appear this phenomenon at 4.5 ms. And the larger the inlet gas flow rate, the shorter the arc re-breakdown time. When the excitation voltage is 3700 V and inlet gas flow rate is 5 m/s, different electrode throat between the electrode maximum temperature change with time is shown in Fig. 5b. When the electrode throat is 2 mm, the temperature will appear to fall and then rise at 2.5 ms. It is caused by the arc re-breakdown. When the electrode throat is 3 mm, it will also appear this phenomenon at 4 ms.It indicates that the smaller the electrode throat, the earlier the arc re-breakdown

occurs. When the electrode throat is 5 mm and inlet gas flow rate is 5 m/s, different excitation voltage between the electrode maximum temperature variation with time is shown in Fig. 5c. The arc temperature is basically not affected by voltage in the range of 3500–4000 V. In order to show the relationship between voltage and arc temperature more clearly, arc temperature changes with the voltage of 1000–4000 V is shown in Fig. 5d. When the voltage is 1000 V, the gas is not breakdown. The temperature of the electrode boundary is also small, indicating that no arc generation at small voltage. When the voltage reaches a certain value, an arc will be generated. And the higher the voltage, the faster the arc temperature reaches a stable value. However, when the voltage exceeds 3500 V, the arc temperature is little affected by the voltage.

The arc re-breakdown phenomenon is shown in Fig. 6. Figure 6a shows the arc temperature distribution cloud when the electrode throat is 5 mm, the excitation voltage is 3700 V, and the inlet gas flow rate is 9 m/s. The temperature of arc plasma presents "arc" distribution. The arc plasma maximum temperature is at the cathode during the arc breakdown stage. And as the arc gradually stabilizes to form an arc column, the maximum value moves to the center of the arc column, and the temperature gradually decreases along the radial direction. A new arc can be seen at 4.7 ms. This is because the fluid has the effect of blowing arc. On the one hand, it can accelerate the heat diffusion and reduce the arc temperature. The original arc temperature drops rapidly before the generation of the new arc channel. On the other hand, it can accelerate the arc elongation process. The arc voltage rapidly increases, causing the arc to re-breakdown. Therefore, in order to obtain a stable arc plasma, the inlet gas flow rate should not be too large, and the electrode throat should not be too small. When the electrode throat is 2 mm, the excitation voltage is 3700 V and the inlet gas flow rate is 5 m/s, arc temperature distribution cloud is shown as Fig. 6b. It can be seen that in the process of arc elongated, the arc burns steadily and the arc column temperature remains basically unchanged. While at the periphery of the arc, the temperature decreases along the radial direction according to a certain gradient under the effect of heat transfer.

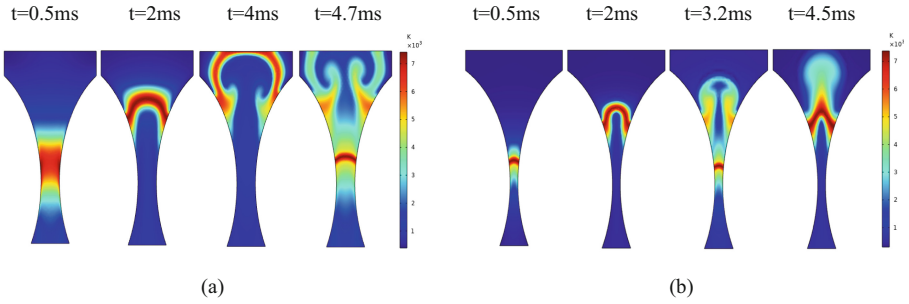

Fig. 6. arc temperature distribution cloud (a) u = 9m/s, U = 3700V, d = 5 mm (b) d = 2 mm, U = 3700V, u = 5 m/s

In addition, this paper investigates the difference of arc starting time under different conditions, seeing Fig. 7. When the excitation voltage is 3700 V and inlet gas flow rate is 5 m/s, different electrode throat corresponding to the arc starting time is shown in Fig. 7a.

The results show that the arc starting time is proportional to the electrode throat spacing when both the excitation voltage and the inlet gas flow rate are fixed. Figure 7b shows the arc starting time corresponding to different excitation voltages when the electrode throat spacing is 5 mm and the inlet gas flow rate is 5 m/s. The results show that the arc starting time is inversely proportional to the excitation voltage when both the electrode throat spacing and the inlet gas flow rate are fixed. From the principle of arc generation, a large number of electrons will be gathered on the cathode plate after applying a certain voltage. Then the electrons fly to the anode at high speed under the action of electric field and strike the argon atoms, thus producing ions and free electrons. Among them, the cations move towards the cathode, and the anions and free electrons move towards the anode. And an arc starts to be generated between the electrodes under the effect of strong collision. Therefore, when the excitation voltage is certain, the shorter the electrode throat, the faster the ions and electrons collide with the cathode, the earlier the arc appears. When the electrode throat is fixed, the higher the voltage, the more electrons the cathode emits under the action of the electric field, the faster the electrons move to the anode direction, thus accelerating the formation of the arc.

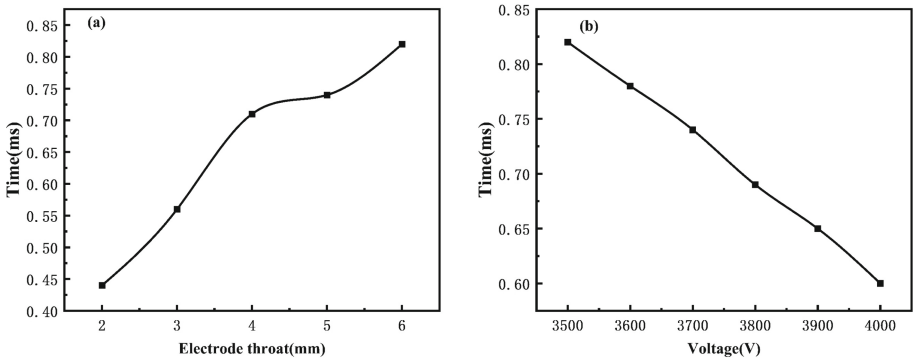

Fig. 7. Arc starting time under different conditions (a) different electrode throats; (b) different excitation voltages

3.4 Electric Field

From $J = \sigma E$, it is known that the current density is approximately proportional to the electric field. And the current density provides energy for the formation of the arc. and it has a large effect on the distribution of arc characteristics [16]. Figure 8 shows the maximum current density between the blade electrodes with time for different inlet gas flow rates, different electrode throats, and different excitation voltages. It can be seen that under different conditions, the current density sharply increases first and then decrease, stabilized at last. The trend can be explained by the arc voltage-current graph. Figure 9 is the arc voltage-current diagram when the inlet gas flow rate is 5 m/s, the electrode throat is 5 mm and the electrode voltage is 3700 V. The arc voltage decreases rapidly at 0.73 ms, the current rises rapidly. The gas is broken down to form an arc. Due to current

density refers to the current per unit area, the arc current density increases rapidly with current. After 0.73 ms, the current density starts to decrease because of the arc current starts to reduce. The arc voltage-current diagram obtained in this paper is consistent with the literature [30], which again verifies the correctness of the model.

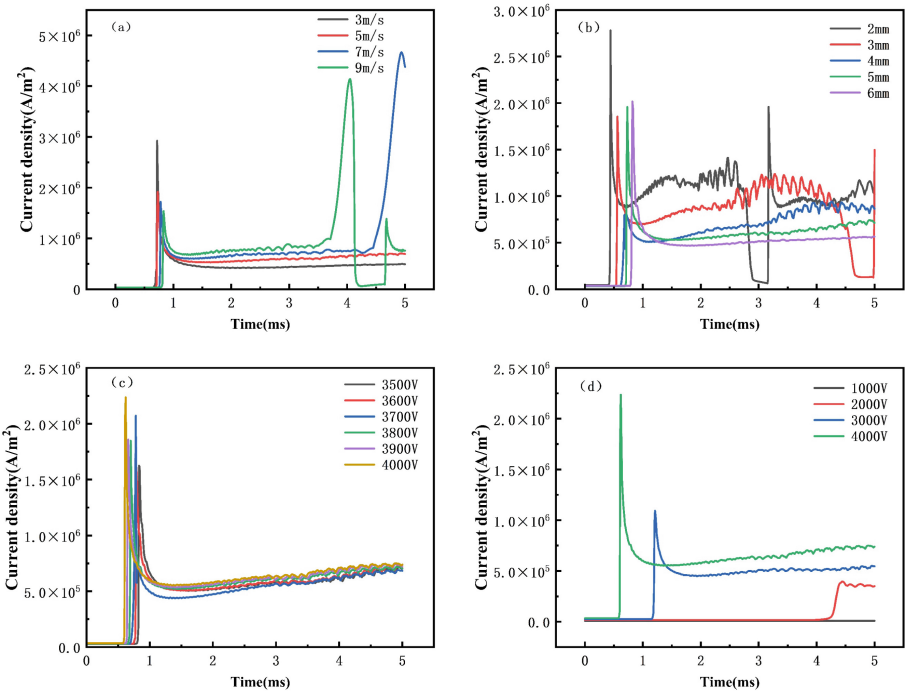

Fig. 8. Plot of maximum current density versus time (a) different inlet gas flow rates (b) different electrode throats (c-d) different voltages

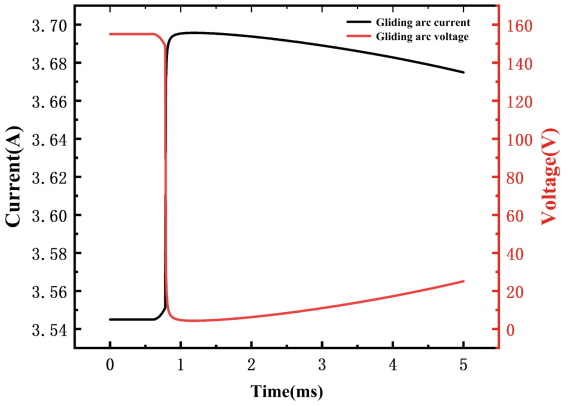

Fig. 9. arc voltage - current diagram, U = 3700 V, d = 5 mm, u = 5 m/s

When the electrode throat is 5 mm and excitation voltage is 3700 V, different inlet flow rate between the electrode maximum current density with time is shown in Fig. 8a. After the current density tends to stabilize, the greater the inlet flow rate, the bigger the current density. The current density of 9 m/s and 7 m/s appears peak at 3.8 ms and 4.8 ms, respectively. This is due to the limitations of the model space structure. Before the arc being blown off, the top of the arc will gather at the exit cross-section. At this time the charge accumulates rapidly. The current density rises rapidly and appears peak. Thereafter, the arc disappearance and re-breakdown at about 4.7 ms. The current density distribution is consistent with the distribution of the first arc start. And this phenomenon also occurs at 7 m/s. When the excitation voltage is 3700 V and inlet gas flow rate is 5 m/s, different electrode throat under the electrode maximum current density changes with time is shown in Fig. 8b. When the electrode throat is 2 mm, the current density trend is the same as the first arc. So as the electrode throat is 3 mm. This is because the arc re-breakdown occurs during this time. When the electrode throat is 5 mm and the inlet gas flow rate is 5 m/s, different excitation voltage between the electrode maximum current density with time is shown in Fig. 8c. The voltage and current density have no obvious relationship. In order to show the relationship between the two more clearly, the voltage range was expanded to 1000–4000 V shown in Fig. 8d. The results shows that the higher the excitation voltage, the higher the current density. The current density is 0 A/m^2 at the excitation voltage of 1000 V. And the gas is not penetrated. There is no conductive path formed in the throat. That is, no arc generation.

In addition, this paper also compares the arc cycle under different inlet gas flow rate and electrode throat spacing at 3700 V, shown as Fig. 10. When the electrode throat spacing is 2 mm and inlet gas flow rate is 5 m/s, the arc cycle is about 2.8 ms. As the inlet gas flow rate increases to 7 m/s, the cycle is correspondingly shortened to about 1.6 ms. Under the condition of fixed voltage and electrode throat spacing, the larger the inlet gas flow rate, the shorter the arc cycle. When the inlet gas flow rate is 7 m/s, the arc cycles of 2 mm and 5 mm electrode throat spacing are 1.6 ms and 5 ms respectively, which shows that the arc cycle shortens as the electrode throat spacing decreases. Therefore, in order to get a stable combustion of the gliding arc, the inlet gas flow rate should not be too large, and the electrode throat spacing should not be too small.

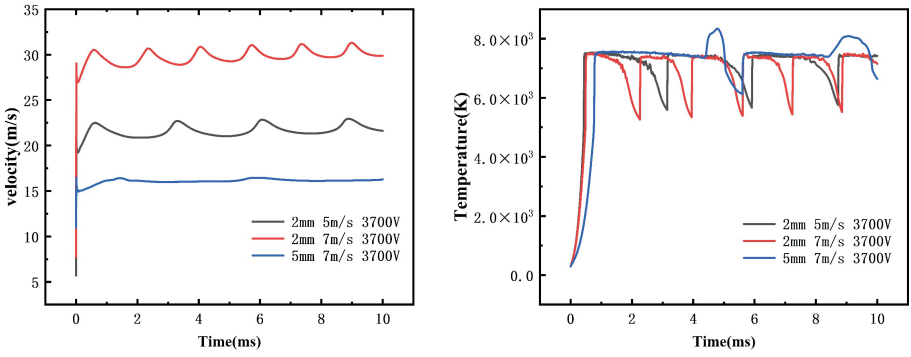

Fig. 10. Different conditions of the arc velocity, temperature and time variation graph

4 Conclusion

In this paper, the argon arc discharge is simulated based on a simplified geometric model with a magneto-hydrodynamic theory, coupled with the electric field equations and considering the gas heat transfer conditions. The conclusions are as follows:

1) The gliding arc discharge presents a cyclic process of arc breakdown, elongation, disappearance and re-breakdown. The arc cycle is correspondingly shortened as the inlet gas flow rate increases and the electrode throat spacing decreases.
2) The inlet air velocity has obvious influence on the arc characteristic distribution. The air velocity drives the arc to glide upward along the electrode, which makes the arc plasma temperature and current density show "arc shape" distribution. The arc plasma temperature and current density are maximum at the cathode during the arc breakdown stage. And as the arc gradually stabilizes to form an arc column, the maximum value moves to the center of the arc column. The temperature and current density gradually decrease along the radial direction.
3) As the flow rate increases, the maximum velocity increases, the temperature and current density decreases. With the narrowing of the electrode throat gap, the temperature and current density reaches the maximum faster. And the smaller the gap, the easier the arc to re-breakdown. The temperature and current density gradually increase with voltage. When the voltage is higher than 3000 V, the change is not obvious.
4) In order to get a stable burning arc, the inlet gas flow rate should not be too large, the electrode throat spacing should not be too small.

References

1. Lu, X.: Plasma jets and their medical applications. High Voltage Technol **37**(06), 1416–1425 (2011)
2. Ma, Y., Zhang, C., Kong, F., et al.: Effect of plasma jet array-assisted thin film deposition on the electrical properties of epoxy resin surface. High Voltage Technol. **44**(09), 3089–3096 (2018)
3. Zhang, R., Xia, Y., Zhou, X., et al.: Effect of He plasma jet treatment on improving the water repellent migration of heavily fouled stained silicone rubber. High Voltage Technol. **43**(12), 3988–3993 (2017)
4. Mei, D.H., Fang, C., Shao, T.: Current status of research on the characteristics and applications of low-temperature plasma at atmospheric pressure. Chinese J. Electric. Eng. **40**(04), 1339–58+425 (2020)
5. Zhang, H., Zhu, F.S., Li, X.D., et al.: Analysis of key technologies for methane reforming by gliding arc discharge plasma. High Voltage Technol. **41**(09), 2930–2942 (2015)
6. Lu, N., Zhang, C.K., Xia, Y., et al.: Research progress of plasma conversion of CO_2. High Voltage Technol. **46**(01), 351–361 (2020)
7. Yao, S.L., Zhang, X.M., Lu, H.: Key technology of low temperature plasma purification of VOCs. High Voltage Technol. **46**(01), 342–350 (2020)
8. Zhang, J.: Research progress of plasma application in the field of energy and environment Safety. Health Environ **21**(10), 1–7 (2021)

9. Chen, J., Shi, Y., Mei, D., et al.: Influence of different gas composition additions on the mode and characteristics of nitrogen gliding arc discharge. High Voltage Technol. 1–10
10. Czernichowski Pure, A.J., Chemistry, A.: Gliding arc: applications to engineering and environment control **66**(6), 1301–1310 (1994)
11. Fridman, A.J.P.C.: Plasma Chemistry (2008)
12. He, L.M., Chen, I., Liu, X.J., et al.: Discharge characteristics of an AC gliding arc at high pressure. High Voltage Technol. **42**(06), 1921–1928 (2016)
13. Lu, N., Sun, D., Wang, B., et al.: Discharge characteristics of AC rotating gliding arc. High Voltage Technol. **44**(06), 1930–1937 (2018)
14. Mei, D., Zeng, Y., Tu, X.: Spectral diagnosis of atmospheric pressure argon gliding arc (in English). High Voltage Technol. **39**(09), 2180–2186 (2013)
15. Wang, Y., Li, X., Yu, Q., et al.: Numerical simulation study of gliding arc low-temperature plasma discharge characteristics. Phys. Lett. **60**(03), 404–410 (2011)
16. Zhao, M., Wang, Y., Yang, S., et al.: Characteristics of multiphysics field distribution in arc plasma. J. Mech. Eng. **58**(08), 153–159 (2022)
17. Liu, X., Liu, C.Y., Zou, J.Y.: Comparative analysis of AC and DC vacuum arc plasma characteristics. J. Vacuum Sci. Technol. **35**(10), 1203–1208 (2015)
18. Chen, W., Chen, L., Liu, C., et al.: Numerical simulation study of DC arc plasma torch Vacuum **56**(01), 56–58 (2019)
19. Bao, J., Yang, Z., Liu, T., et al.: Numerical simulation study of the temperature field of vacuum free-burning helium arc **43**(4), 4 (2006)
20. Hui, L.S., Trelles, J.P., Murphy, A.B., et al.: Numerical simulation of the flow characteristics inside a novel plasma spray torch (2019)
21. Trelles, J.P., Pfender, E., Heberlein, J.J.P.C., et al.: Multiscale Finite Element Modeling of Arc Dynamics in a DC Plasma Torch **26**(6), 557–575 (2006)
22. Jian, X.,Wu, C.S.: Numerical analysis of the coupled arc-weld pool-keyhole behaviors in stationary plasma arc welding - ScienceDirect **84**, 839–847 (2015)
23. Chen, H.: Research on plasma flow characteristics of arc heating. Nanjing University of Technology (2014)
24. Tu, X., Gallon, H.J., Whitehead, J.C.: Dynamic Behavior of an Atmospheric Argon Gliding Arc Plasma. **39**(11), 2900–2901 (2011)
25. Zhang, R., Luo, G., Huang, H., et al.: The law of influence of electrode structure on the size of gliding arc discharge plasma **45**(10), 8 (2019)
26. Feng, L.-W.: Simulation of flow in expansion tubes and its local loss control. Technol. Market **26**(11), 57–58 (2019)
27. Guo, J., Liu, J., Yan, X., et al.: Two-dimensional numerical simulation of plasma discharge characteristics of DC arc plasma jet method based on FLUENT software. J. Vacuum Sci. Technol. **36**(03), 312–318 (2016)
28. Liu, Y., Wu, G., Guo, Y., et al.: Analysis of DC arc motion characteristics of the inviting arc angle electrode. J. Southwest Jiaotong Univ. 1–8
29. Zhong, Y.M.: MHD model simulation of small-current DC air arc and its experimental study. Chongqing University (2020)
30. Cheng, W.: Study of high voltage DC air discharge model. Nanjing University of Aeronautics and Astronautics (2018)